Predicting the prevalence of genetic trade-offs among adaptive substitutions

Tim Connallon[1†], Peter Czuppon[2], Colin Olito[3], Debora Goedert[4], Hanna Kokko[5,6], Angela Nava-Bolaños[7], Sofie Nilén[3], Erik I Svensson[3], Martyna Zwoinska[8], Ludovic Dutoit[9*], Filip Ruzicka[10*]

[1] School of Biological Sciences, Monash University, Australia

[2] Institute for Evolution and Biodiversity, University of Münster, Germany

[3] Department of Biology, Lund University, Sweden

[4] Norwegian University of Science and Technology, Norway

[5] Institute of Organismic and Molecular Evolution, The Johannes Gutenberg University Mainz, Germany

[6] Institute for Quantitative and Computational Biosciences, The Johannes Gutenberg University Mainz, Germany

[7] Unidad Multidisciplinaria de Docencia e Investigación, Universidad Nacional Autónoma de México, México

[8] Department of Ecology and Genetics, Uppsala University, Sweden

[9] Department of Zoology, University of Otago, New Zealand

[10] Institute of Science and Technology Austria, Austria

[*] Equal contributions

[†] Corresponding author: tim.connallon@monash.edu

Abstract

Genetic trade-offs—which occur when variants that are beneficial in some contexts of natural selection are harmful in others—can influence a wide range of evolutionary phenomena, from the maintenance of genetic variation to the evolution of aging and sex differences. An extensive body of evolutionary theory has focused on the consequences of such trade-offs, and recent analyses of Fisher's geometric model have further quantified the expected proportion of *new* mutations that exhibit trade-offs. However, the theory remains silent regarding the prevalence of trade-offs among the variants that contribute to adaptation. Here, we extend Fisher's geometric model to predict the prevalence of trade-offs among the adaptive mutations that become established or fixed in a population. We consider trade-offs between sexes, habitats, fitness components, and temporally fluctuating environments. In all four scenarios, trade-off alleles are consistently under-represented among established relative to new beneficial mutations—an effect that arises from the greater susceptibility of trade-off alleles to genetic drift. Adaptation during a population size decline exacerbates this deficit of trade-offs among established mutations, whereas population expansions dampen it. Consequently, threatened populations should primarily adapt using unconditionally beneficial alleles, while invasive populations are more prone to adaptation using variants that exhibit trade-offs.

Keywords: adaptation, pleiotropy, sexual conflict, trade-offs

Introduction

Genetic trade-offs—in which alleles with a fitness advantage in one context of selection are costly when expressed in others—play important roles in a wide range of evolutionary phenomena, including the evolution of ecological niche breadth (Futuyma and Moreno 1988), local adaptation (Hereford 2009), costs of resistance to antibiotics and pesticides (*e.g.*, Lenormand et al. 2018; Mangan et al. 2023), the maintenance of genetic variation in life-history traits (Charlesworth and Hughes 2000; Flatt 2020), ageing and senescence (Williams 1957; Kreider et al. 2021), the evolution of species with complex life cycles (Moran 1994; Aguirre et al. 2014), and the evolution of sexes and sex differences (Charlesworth and Charlesworth 1978; Lande 1980; Connallon and Clark 2014a; Pennell et al. 2024). However, many of these phenomena can arise in the absence of trade-offs. For instance, senescence can result from the accumulation of late-acting deleterious alleles rather than from genetic trade-offs between early and late life (the antagonistic pleiotropy theory), two non-exclusive evolutionary explanations for the evolution of ageing (Medawar 1952; Lehtonen 2020; Lemaître et al. 2024). Similarly, a large fraction of genetic variation in life-history traits is likely due to unconditionally harmful mutations maintained by mutation-selection balance (Haldane 1937; Charlesworth 2015). Other examples include the evolution of cost-free specialisation, resistance, or local adaptation (Fry 1996, Kawecki and Ebert 2004; Anderson et al. 2013). Evaluating the evolutionary importance of trade-offs therefore requires a combination of theory that links pattern to process and empirical tests that unambiguously distinguish between hypotheses that do, and do not, invoke trade-offs.

Advances in genomics, and its application to most areas in contemporary biology, have produced an impressive catalogue of genetic trade-offs between different contexts of selection. In addition to famous, pre-genomics cases such as industrial melanism (a trade-off in predator avoidance between visual environments: Cook 2003) and sickle-cell anaemia (disease resistance trading off with blood circulation: Aidoo et al. 2002), we now know of numerous genetic variants that exhibit trade-offs. Examples include seasonally varying selection for different genetic variants in *Drosophila* (Bergland et al. 2014; Bitter et al. 2024), trade-offs between survival and male mating success in Soay sheep (Johnston et al. 2013), and

'sexually antagonistic' variants that benefit one sex at a cost to the other (see Barson et al 2015; Ruzicka et al. 2019, 2022; Rusuwa et al. 2022; Glaser-Schmitt et al. 2024). These examples are far from exhaustive, as a dive into the evolutionary genetics literature quickly reveals.

On the theory side, there has been extensive mathematical analysis of the population genetic dynamics of trade-offs, beginning with the assumption that trade-offs exist and then proceeding to work out the evolutionary consequences of that assumption (reviewed in Prout 2000; Connallon and Hall 2018). Moreover, the resurrection of Fisher's geometric model in recent years (Fisher 1930, pp. 38-41; Orr 1998; Tenaillon 2014) has provided a convenient framework for predicting the phenotypic and fitness effects of mutations, rather than arbitrarily assigning fitness effects to genotypes (reviewed in Orr 2005a,b; Tenaillon 2014; Connallon and Hodgins 2021). Studies based on Fisher's geometric model have addressed a broad range of questions related to the genetics of adaptation, spanning the distribution of fitness effects of spontaneous mutations (Martin and Lenormand 2006a,b; 2015; Manna et al. 2011), the phenotypic and fitness effects of adaptive genetic polymorphisms and substitutions (Orr 1998; Martin and Lenormand 2006a,b; 2008; Kopp and Hermisson 2009; Sellis et al. 2011; Matuszewski et al. 2014; McDonough and Connallon 2023), and questions about arms races (Scott and Queller 2019), social traits (Gardner 2024), evolutionary rescue (Anciaux et al. 2019; Osmond et al. 2020; Mohammadi and Campos 2025), and speciation (Schneemann et al. 2024).

Genetic theories of adaptation, aided by the resurgence of Fisher's geometric model, have nevertheless overlooked the potentially important role of trade-offs to *adaptive divergence*. Several extensions of Fisher's geometric model have shown that trade-offs readily emerge among *new* mutations across ecological, social, or developmental environments (Moorad and Promislow 2008; Moorad and Hall 2009; Martin and Lenormand 2015; Connallon and Clark 2014a, 2014b), leading to genetic constraints on the rate of adaptation in complex environments (Martin and Lenormand 2015; Marshall and Connallon 2023). However, only a subset of new mutations will ultimately contribute to adaptive divergence, as some are eliminated by natural selection and others are lost by chance despite having net positive fitness effects

(*e.g.*, Haldane 1927; Kimura 1962; Otto and Whitlock 1997). Thus, while previous theory yields clear predictions about the prevalence of trade-offs among new mutations (Martin and Lenormand 2015) and their consequences for the overall rate of evolutionary change (see Fig. 6 of Martin and Lenormand 2015; Marshall and Connallon 2023), we still lack clear predictions regarding the fraction of the alleles contributing to adaptive divergence that exhibit trade-offs. Do mutations exhibiting trade-offs between environments, fitness components, or sexes often contribute to adaptive divergence, or are they more likely to become lost due to purifying selection or genetic drift? How do specific features of selection, the environment, and/or population demography influence the proportion of adaptive substitutions that exhibit trade-offs?

Here, we use Fisher's geometric model to study the prevalence of trade-offs among new mutations and among the subset of new mutations that contributes to adaptation. In our models, trade-offs arise because of differences in selection between sexes, habitats, temporally alternating environments, and fitness components. We first quantify the extent of fitness trade-offs among the new mutations that can potentially contribute to adaptation (*i.e.*, mutations whose fitness effects yield a net benefit when averaged across the contexts of selection). We then consider the extent of trade-offs among the mutations that do contribute to adaptation (*i.e.*, mutations that become established). Given previous theory highlighting how changes in population size influence the genetic variants that contribute to adaptation (see Otto and Whitlock 1997; Osmond et al. 2020; Yamaguchi and Otto 2022; McDonough and Connallon 2023), we further explore the prevalence of trade-offs in populations that are demographically stable versus those that undergo episodes of population growth (*e.g.*, invasive species) or decline (*e.g.*, declines that either stabilise or precede bouts of evolutionary rescue). Our analysis shows that these demographic scenarios substantially influence the pervasiveness of genetic trade-offs among the alleles contributing to adaptive evolution.

The Models

Overview of the models

Our models focus on haploid populations with discrete generations. As in previous analyses of Fisher's geometric model (*e.g.*, Orr 2005a, 2005b; Tenaillon 2014), we assume that adaptation is based on the sequential establishment of new beneficial mutations (rather than standing genetic variation), with beneficial mutations arising at sufficiently low rates that their establishment probabilities are independent of one another. Such populations evolve by "adaptive walks" whose steps each involve the origin and spread of a new beneficial variant (Maynard Smith 1970; Gillespie 1984; Orr 1998; McCandlish and Stoltzfus 2014). This mutation-limited view of adaptation is relevant to trait systems where the total mutation rate is small (*i.e.*, $NU << 1$, where N is the population size and U is the average number of new mutations, per haploid genome, that affect the traits), or where phenotypic dimensionality is sufficiently high that the mutation rate to *adaptive* alleles is small (*i.e.*, $NU_b << 1$, where U_b is total mutation rate to beneficial alleles). Various lines of evidence from molecular evolutionary studies of protein sequence adaptation support the adaptive walk and mutation-limited scenarios of adaptation (Rousselle et al. 2020; Moutinho et al. 2022; McDonough et al. 2024). However, the extent to which adaptation is mutation limited is unclear, and we later discuss how our predictions might change in cases where adaptation uses standing genetic variation.

Our main analysis predicts the probability that an individual step during adaptation involves a trade-off, and we identify aspects of population size dynamics and the geometry of selection that influence the prevalence of trade-offs among new mutations and adaptive substitutions. The population size during a single step of adaptation is assumed to be either stable (constant in size), geometrically growing, or geometrically declining, though we relax these assumptions in our simulations by including density regulation, which forces the population to stabilise in size. As we elaborate in the Discussion, our single step results, when coupled with previous predictions about how the geometry of selection changes during

adaptive walks (Connallon and Clark 2014a; Martin and Lenormand 2015; Marshall and Connallon 2023), yield clear predictions about the relative importance of trade-offs across different phases of an adaptive walk.

Each population is assumed to experience selection in two fitness contexts, each contributing equally to the evolutionary response. We consider four specific trade-off scenarios (Model 1a, 1b, 2a and 2b) that encompass two distinct dynamics of allele frequency change (Model 1 vs. Model 2). The four scenarios match those in Prout (2000), excepting meiotic drive, which we do not cover. Our four selection scenarios are:

- ***Sex differences in selection (Model 1a)*:** In this model, allele frequencies are identical between the sexes at the start of each generation. Sex differences in selection lead to divergence in allele frequencies between the females and males that contribute to reproduction. The pool of breeding females and males mate randomly to produce diploid zygotes that immediately undergo meiosis and yield haploid individuals of each sex that comprise the next generation (see Kidwell et al. 1997; Gregorius 1982; Connallon et al. 2019).
- ***Differences in selection between a pair of habitats (Model 1b)*:** In each generation, offspring randomly settle across two equally abundant habitat types. After viability selection, each habitat contributes 50% of the pool of breeding adults that produce the offspring of the next generation. This scenario is a special case of Levene's model of selection across multiple niches (Levene 1953; Christiansen 1975), which in our case involves two equally abundant niches, there is high migration among habitat patches (as in Levene 1953), and each habitat type produces an equal number of breeding adults in each generation. Under these assumptions, the allele frequency dynamics are identical to those of Model 1a.

- ***Multiplicative fitness components (Model 2a)*:** Selection occurs through two major fitness components that combine multiplicatively to determine total fitness (*e.g.*, preadult survival and fecundity), as in previous models of antagonistic pleiotropy (Curtsinger et al. 1994). Such scenarios may involve pleiotropic trade-offs between fitness components expressed in the same or in different life-history stages, including stages separated by metamorphosis (though metamorphosis may limit pleiotropy between stages; Goedert and Calsbeek 2019).
- ***Temporally alternating environments (Model 2b)*:** Two environments of selection predictably oscillate between generations. This is a special case of a much broader array of evolutionary models involving temporally fluctuating selection (see Felsenstein 1976; Wittmann et al. 2023). In both Models 2a and 2b, net selection is multiplicative across the pair of selection contexts. However, while both contexts occur within a single generation in Model 2a, they occur over two generations in Model 2b. Thus, the allele frequency dynamics of Models 2a and 2b are equivalent provided time is rescaled between the scenarios (see below).

While it is possible that all four trade-off scenarios might arise in single populations, for simplicity we analyse each scenario separately.

Evolutionary dynamics

Considering a single polymorphic locus at a time, the deterministic evolutionary dynamics of a mutant allele *A* (the resident allele is *a*), can be described as follows. For Models 1a and 1b, the expected change in frequency of the *A* allele, per generation, is:

$$\Delta p = \frac{pq}{2}\left(\frac{s_1}{1+ps_1} + \frac{s_2}{1+ps_2}\right) \quad (1)$$

where p is the frequency of allele A, q is the frequency of allele a, and s_1 and s_2 are the selection coefficients for the A allele in contexts 1 and 2, respectively (*i.e.*, s_1 and s_2 refer to the sexes 1 and 2 in Model 1a, and to habitats 1 and 2 in Model 1b). The equivalent of eq. (1) can be found in previous haploid models of sex differences in selection (Connallon et al. 2019) and multiple-niche polymorphism (Gliddon and Strobeck 1975). Note that the selection coefficients are subject to the constraints: $s_1 > -1$ and $s_2 > -1$, with negative values indicating that A is deleterious in the given selection context and positive values indicating that A is beneficial. Trade-offs occur when the selection coefficients have opposite signs between contexts ($s_1 < 0 < s_2$, or $s_2 < 0 < s_1$). The *net selection coefficient* for a rare A allele is $s = (s_1 + s_2)/2$.

The evolutionary dynamics for Models 2a and 2b (fitness components or temporally alternating environments) are described by:

$$\Delta p = \frac{pq(s_1 + s_2 + s_1 s_2)}{1 + p(s_1 + s_2 + s_1 s_2)} \quad (2)$$

with p, q, s_1 and s_2 defined as before. Here, the net-selection coefficient for a rare mutant allele is $s = s_1 + s_2 + s_1 s_2 \approx s_1 + s_2$, which is based on the algebraic expansion of the net fitness effect of the A relative to the a allele (*i.e.*, the fitness of A relative to a is $w_A = (1 + s_1)(1 + s_2) = 1 + s_1 + s_2 + s_1 s_2$; Crow & Kimura 1970, p.185), with the final approximation applicable for variants whose fitness effects are small (*i.e.*, terms of $s_1 s_2$ contribute negligibly to s when $|s_1|$ and $|s_2| << 1$). Note that eq. (2) predicts the evolutionary dynamics for Models 2a and 2b, but the timescale differs between the two scenarios, with Δp describing change over a single generation in Model 2a and Δp representing change across two generations in Model 2b. Eq. (2) is a special case of earlier models in which the different episodes of selection that arise within or across generations combine multiplicatively to determine evolutionary dynamics (Dempster 1955; Arnold and Wade 1984).

The establishment probabilities of rare mutations are determined by their net selection coefficients. Following Otto and Whitlock (1997), the establishment probability of a net beneficial mutant allele can be approximated as:

$$\Pr(\text{est.}|s > 0) \approx 2\big((1+s)R - 1\big) \quad (3)$$

where $s = (s_1 + s_2)/2$ in Models 1a and 1b, $s \approx s_1 + s_2$ in Models 2a and 2b, and R is the reproductive factor of the population ($R = 1$ in populations of constant size, $R > 1$ in expanding populations, and $0 < R < 1$ in declining populations). Eq. (3), which we use in our analytical models, is valid when $\max(0, (1-R)/R) < s < 0.1$ (Otto and Whitlock 1997; McDonough and Connallon 2023). While net deleterious mutations can also go to fixation in finite populations (see Supplementary Material Appendix 4), our primary focus is on adaptation, and we thus emphasize adaptive genetic variants in our analyses.

Selection coefficients from Fisher's geometric model

Values of s_1 and s_2 for random mutations are easily generated using Fisher's geometric model (Martin and Lenormand 2015) and the process of generating them is the same for each trade-off scenario. We use the 'isotropic' version of Fisher's model (Fisher 1930; Orr 1998; Tenaillon 2014), in which there are n pleiotropically linked traits under mutation and selection, mutation orientations are random in multidimensional space, and fitness of each genotype is a Gaussian function of the Euclidean distance between its phenotype and the optimum (Fig. 1 provides a conceptual overview of the basic elements of the model, using an example of $n = 2$ traits).

{Figure 1}

Let the vector **A** represent the phenotype of the resident genotype and vectors $\mathbf{O_1}$ and $\mathbf{O_2}$ represent the optima in selection environments 1 and 2, respectively (see Fig. 1). The Euclidean distances to the optima are $z_1 = \sqrt{\sum_i^n (O_{1,i} - A_i)^2}$ and $z_2 = \sqrt{\sum_i^n (O_{2,i} - A_i)^2}$, where i subscripts denote positions within

the vectors **A**, $\mathbf{O_1}$, and $\mathbf{O_2}$ (*e.g.*, $i = 1$ would denote the first of the n positions in a given vector). Mutations affect the expression of each trait. The phenotype associated with a random mutant allele is $\mathbf{A}_{mut} = \mathbf{A} + \mathbf{M}$, where **M** is a vector of the trait-specific effects of the mutation. The elements of **M**, which represent the phenotypic effects of the mutation on each of the n traits, are independent draws from a normal distribution with mean of zero and standard deviation of m. The distances of a mutant phenotype to each optimum are $z_{1,mut} = \sqrt{\sum_i^n \left(O_{1,i} - A_i - M_i\right)^2}$ and $z_{2,mut} = \sqrt{\sum_i^n \left(O_{2,i} - A_i - M_i\right)^2}$, and the selection coefficients are $s_1 = \exp\left(\frac{1}{2}\left(z_1^2 - z_{1,mut}^2\right)\right) - 1$ and $s_2 = \exp\left(\frac{1}{2}\left(z_2^2 - z_{2,mut}^2\right)\right) - 1$.

As previously shown by Martin and Lenormand (2015), when dimensionality is reasonably high (*e.g.*, $n > 10$) and the population is displaced from its optima, then distributions of selection coefficients for a pair of environments are approximately bivariate normal; the marginal mean and variance in environment j ($j \in \{1, 2\}$) are $\bar{s}_j = -\frac{1}{2}nm^2$ and $\sigma_j^2 = m^2\left(z_j^2 + \frac{1}{2}nm^2\right)$, respectively, and the covariance is $\mathrm{cov}(s_1, s_2) = m^2\left(z_1 z_2 \cos(\theta_{sel}) + \frac{1}{2}nm^2\right)$, where θ_{sel} is the angle between multivariate orientations of selection to each optimum ($0 \leq \theta_{sel} \leq \pi$). Note that θ_{sel} values of zero, $\pi/2$ and π correspond to identical, orthogonal, and completely opposing orientations of selection, respectively. Fig. 1A shows an example where $\theta_{sel} = \pi/3$, which corresponds to an angle of 60 degrees. We base our analytical and numerical results on the bivariate normal approximation and use exact distributions of selection coefficients in our simulations.

As illustrated in Fig. 1, whether a mutation is favoured in a context of selection depends on whether it shifts the phenotype of its carriers closer to the optimum. The pair of circles show the phenotypic states that are adaptive in each of the two environments of selection. Mutations producing phenotypes outside of both circles are deleterious in both environments, while those that fall within both circles are unconditionally beneficial (blue dots). Mutations exhibit trade-offs when they are harmful in one context of selection and beneficial in the other, though only a subset of trade-off mutations have net positive effects (orange dots); the remainder of trade-off mutations are net-deleterious (*i.e.*, $s_1 s_2 < 0$ and $s_1 + s_2 < 0$, which correspond to

the grey dots that fall within one circle but not the other). Mutations with net positive effects (which meet the condition $s_1 + s_2 > 0$, with or without a trade-off) can potentially contribute to adaptation while those with net deleterious effects (those with $s_1 + s_2 < 0$) cannot.

Although our primary analysis follows Martin and Lenormand (2015) in assuming that the effects of mutations on the n traits follow a multivariate normal distribution, we also present results that are conditioned on a given mutation size (results for fixed values of $\|\mathbf{M}\|$ are presented in Supplementary Material Appendix 1), which yield qualitatively similar predictions to our main analysis. We therefore expect our qualitative results to be robust to the specific distribution of mutational magnitudes, which is unknown and varies among studies using Fisher's model (*e.g.*, Orr 1998; Martin and Lenormand 2015; McDonough and Connallon 2023).

Analysis of the model

Full details underlying our main mathematical results are provided in the Supplementary Material; we present the most important results in the main text. Since the mathematical results rely on approximations for the distribution of selection coefficients and probabilities of establishment of new mutant alleles, we have also carried out exact simulations of the origin and establishment of new mutations. In these simulations, we introduce one mutant allele at a time, define its phenotypic effect and selection coefficients in each environment using Fisher's geometric model, and characterize its evolutionary fate (establishment or loss) via Wright-Fisher forward simulations. Each allele is initiated at a starting frequency of $1/N$, where N is the effective population size. A mutation was regarded as "established" if it was favoured by selection ($s > 0$) and reached a frequency that matched or exceeded its deterministic equilibrium. In Models 1a and 1b (sex- and habitat-specific selection), which can lead to balanced polymorphism or adaptive substitutions, the stable deterministic equilibrium for a net beneficial mutation is $\hat{p} = 1$ in cases where the mutation is favoured to fix (*i.e.*, when $0 < s_1 + s_2 > -2s_1s_2$, which follows from a linear stability analysis of eq. (1)),

and otherwise the stable equilibrium is polymorphic with frequency $\hat{p} = -(s_1 + s_2)/(2s_1s_2)$ (the polymorphic equilibrium is valid when $0 < s_1 + s_2 < -2s_1s_2$). Models 2a and 2b (multiplicative fitness components and temporally alternating environments) do not permit balanced polymorphism, and the stable equilibrium for a net beneficial mutation is always $\hat{p} = 1$. We have carried out full stochastic forward simulations for Models 1a and 1b. We rely on numerical methods to compare the predictions of Models 1a and 1b with those of Models 2a and 2b.

All simulations were carried out in R (R Core Team 2021). The associated code is archived at the link: https://doi.org/10.5281/zenodo.15036232.

Results

Preliminary comments

Two factors generate trade-offs in our models (Fig. 1). Trade-offs can arise (*i*) when the direction of selection differs between contexts of selection (cases where $\theta_{sel} > 0$) and/or (*ii*) when the magnitudes of population displacements from the optima differ between selection contexts (cases where $z_1 \neq z_2$). To characterise how each factor contributes to the emergence of trade-offs, we initially present results for each in isolation (see the limiting cases in Fig. 1B) and then generalize to cases where both factors occur simultaneously ($\theta_{sel} > 0$ and $z_1 \neq z_2$). For simplicity, we provide a comprehensive overview of fitness trade-offs in models of sex- and habitat-specific selection (Models 1a and 1b, described above), and later outline parallels with models involving different fitness components and temporally oscillating environments (Models 2a and 2b).

Limiting Case 1: Equal displacements from the optima, different selection orientations

Under sex- or habitat-specific selection (Models 1a and 1b) with the resident genotype equally maladapted between environments (*i.e.*, $z = z_1 = z_2$; Fig. 1), the probability that a net-beneficial mutation with fitness effect s exhibits a trade-off is:

$$\Pr(\text{trade-off} \mid s) = 1 - \operatorname{erf}\left(\frac{s}{mz\sqrt{1-\cos(\theta_{sel})}}\right) \tag{4}$$

(see eq. (S3) in the Supplementary Material) where *erf* refers to the error function, m is the standard deviation of the phenotypic effects of mutations on each trait, and $\cos(\theta_{sel})$ measures the correlation between orientations of selection in each environment ($\cos(\theta_{sel}) = 1$ and thus $\theta_{sel} = 0$, represents a perfect alignment of selection between environments; $\cos(\theta_{sel}) = 0$ corresponds to orthogonal directions of selection; see Fig. S6 for illustrations of how $\cos(\theta_{sel})$ and θ_{sel} relate to the geometry of selection). An example of the distribution of fitness effects and the proportion of net beneficial mutations exhibiting trade-offs is shown in Fig. 2A. Eq. (4) implies, and Fig. 2A confirms, that the probability of a trade-off decreases as the net benefit of the mutation (s) increases. Consequently, trade-offs are enriched among mutations with weakly beneficial effects and deficient among mutations with strongly beneficial effects.

{Figure 2}

To obtain the *total* probability with which net-beneficial variants exhibit trade-offs, we integrate the conditional probability (eq. (4)) over the distribution of s for net-beneficial mutations, which yields:

$$\Pr(\text{trade-off} \mid s > 0) \approx 1 - \frac{\int_0^\infty \operatorname{erf}\left(\frac{s}{mz\sqrt{1-\cos(\theta_{sel})}}\right) \exp\left(-\frac{(s-\bar{s})^2}{2\sigma^2}\right) ds}{\sqrt{\frac{\pi\sigma^2}{2}}\left(1 + \operatorname{erf}\left(\frac{\bar{s}}{\sqrt{2\sigma^2}}\right)\right)} \tag{5}$$

where $\bar{s} = -\frac{1}{2}nm^2$ denotes the mean and $\sigma^2 = \frac{1}{2}m^2\left((1+\cos(\theta_{sel}))z^2 + nm^2\right)$ is the variance of s for random mutations (see the Supplementary Material). While there is no closed-form solution for eq. (5), a comparison of numerical evaluations with simulations shows that eq. (5) accurately predicts the proportion of new beneficial mutations that exhibit trade-offs (Fig. 2B). The numerical results and simulations suggest that trade-offs increase in prevalence as *n* and *m* increase (implying a cost of complexity; Orr 2000; Wang et al. 2010), and they decrease in prevalence with increasing distance to the optimum and/or increased alignment of phenotypic selection across environments (*i.e.*, as *z* and/or $\cos(\theta_{sel})$ increase; see Fig. 2B, which illustrates the effect of $\cos(\theta_{sel})$; additional numerical and simulation results can be found in Fig. S4 and in the Mathematica notebook presented in the Supplementary Material).

For a mutation to contribute to adaptation, it must both improve fitness and avoid loss due to genetic drift. Although a substantial fraction of new, net beneficial mutations exhibit trade-offs when the directions of phenotypic selection are misaligned between environments (*i.e.*, $\cos(\theta_{sel}) < 1$), net-beneficial mutations that exhibit trade-offs tend to be weakly advantageous (as implied by eq. (4) and illustrated in Fig. 2A), making them more susceptible to loss by drift than beneficial mutations without trade-offs. Among the mutations that successfully establish in the population (*i.e.*, those that are both beneficial and not lost by drift), the proportion exhibiting a trade-off is:

$$\Pr(\text{trade-off} \mid \text{established}) \approx 1 - \frac{\int_{s_{\min}}^{\infty} \operatorname{erf}\left(\frac{s}{mz\sqrt{1-\cos(\theta_{sel})}}\right)\left((1+s)R-1\right)\exp\left(-\frac{(s-\bar{s})^2}{2\sigma^2}\right)ds}{\int_{s_{\min}}^{\infty}\left((1+s)R-1\right)\exp\left(-\frac{(s-\bar{s})^2}{2\sigma^2}\right)ds} \quad (6)$$

where $s_{\min} = \max(0, (1-R)/R)$ is the minimum benefit of mutations that potentially contribute to adaptation, and *R* is the reproductive factor of the population ($R > 1$ is expanding; $R = 1$ is stable; $R < 1$ is declining).

Numerical evaluation of eq. (6) and stochastic simulations show that trade-offs are consistently less common among established relative to new, net-beneficial mutations (Fig. 2B). Moreover, the population

size dynamics that occur during adaptation modify the magnitude of this discrepancy. Trade-offs are particularly common among alleles contributing to adaptation in growing populations, whereas they are deficient in declining populations (adaptation in stable-sized populations show an intermediate pattern). These effects of population size dynamics are substantial and occur under quite moderate rates of population size change. Growth of a few percent of the population size, per generation, leads to a similar proportion of trade-offs in established and new adaptive mutations. In contrast, population declines of a few percent or less, per generation, largely remove trade-offs from the pool of variants contributing to adaptation.

Limiting Case 2: Unequal displacements from the optima, same selection orientations

Under sex- or habitat-specific selection (Models 1a and 1b) with perfect alignment in the direction of selection (*i.e.*, $\cos(\theta_{sel}) = 1$ or $\theta_{sel} = 0$; see Fig. 1), trade-offs will still arise when maladaptation is more severe in one environment relative to the other. Here, trade-off proportions become simple functions of dimensionality (n), the sizes of mutational effects per trait (m), and the distance to each optimum ($z_{\min}$ and $z_{\max}$ and their average, $\bar{z} = (z_{\min} + z_{\max})/2$; see Fig. 3A). The probability that a new net beneficial mutation exhibits a trade-off is:

$$\Pr(\text{trade-off} \mid s > 0) \approx \frac{\operatorname{erf}(x_{\min}/\sqrt{2}) - \operatorname{erf}(\bar{x}/\sqrt{2})}{1 - \operatorname{erf}(\bar{x}/\sqrt{2})} \quad (7)$$

where $x_{\min} = nm/\left(2\sqrt{z_{\min}^2 + nm^2/2}\right)$ and $\bar{x} = nm/\left(2\sqrt{\bar{z}^2 + nm^2/2}\right)$ represent the average scaled sizes (respectively) for random mutations in the environment closest to the optimum ($x_{\min}$) and in the average environment ($\bar{x}$). These scaled sizes are conceptually similar to those from previous versions of Fisher's geometric model (Fisher 1930; Orr 1998; see Supplementary Material Appendix 1).

The probability of trade-offs among mutations that establish in a population of constant size is:

$$\Pr(\text{trade-off} \mid \text{established}) \approx$$

$$\frac{\frac{\sqrt{2}}{\sqrt{\pi}}\left(\exp\left(-\frac{1}{2}\bar{x}^2\right)-\exp\left(-\frac{1}{2}x_{\min}^2\right)\right)+\bar{x}\left(\operatorname{erf}\left(\frac{\bar{x}}{\sqrt{2}}\right)-\operatorname{erf}\left(\frac{x_{\min}}{\sqrt{2}}\right)\right)}{\frac{\sqrt{2}}{\sqrt{\pi}}\exp\left(-\frac{1}{2}\bar{x}^2\right)-\bar{x}\left(1-\operatorname{erf}\left(\frac{\bar{x}}{\sqrt{2}}\right)\right)} \quad (8)$$

with the more complicated expressions for cases of population growth or decline presented in the Supplementary Material (see eqs. (S17) and (S18)). The analytical predictions compare well to simulations, provided the phenotypic effect sizes of new mutations are small relative to the mean distance to the optimum (i.e., $m\sqrt{n} \ll \bar{z}$), and they otherwise underestimate the true probability of trade-offs (see Fig. 3).

Trade-offs among new adaptive mutations and established mutations are rare when asymmetries in the displacements from the optima are weak ($z_{\min} \approx z_{\max} \approx \bar{z}$ *vis* $z_{\min}/\bar{z} \approx 1$) and/or mutational effects are small relative to the distance to the optimum ($m\sqrt{n}/\bar{z} \approx 0$) (Fig. 3), and they become common when displacements show pronounced asymmetries and mutational effects are large relative to the distance to the optimum. These effects arise because mutations have a relatively high probability of being beneficial in contexts where the population is more severely maladapted (Fisher 1930), whereas most or all mutations are deleterious in the well-adapted contexts. Asymmetries in the opportunity for evolutionary improvement in each context can therefore lead to extensive trade-offs, despite alignment of the direction of selection. Established mutations are again less likely to show trade-offs than new adaptive mutations (Fig. 3), which reflects the weaker net fitness effects of trade-off alleles relative to mutations that are unconditionally beneficial. Effects of population size change remain the same as before, where trade-offs are more common among the mutations that become established in growing relative to declining populations (see Fig. 4B).

{Figure 3}

Unequal displacements from the optima and different selection orientations

The results presented above predict trade-offs due to the isolated effects of different orientations of selection between environments ($\theta_{sel} > 0$), or different magnitudes of displacement from the optimum of each environment ($z_1 \neq z_2$). More general expressions for trade-off probabilities under arbitrary displacements from the optima and orientations of selection are presented in the Supplementary Material (eqs. (S10-S12)). Unsurprisingly, trade-off probabilities systematically increase when both the displacements from the optima and orientations of selection differ between environments (i.e., $\cos(\theta_{sel}) < 1$ and $z_1 \neq z_2$; see Fig. 4 and Fig. S5). All other factors—including mutant phenotypic effect sizes (m), the mean distance from the optima ($\bar{z} = (z_1 + z_2)/2$), and changes in population size—have the same effects on the prevalence of trade-offs as already described.

{Figure 4}

Comparison of the different trade-off models

There are two key differences between the trade-off scenarios that we have considered so far (sex- and habitat-specific selection; Models 1a and 1b), and trade-offs between fitness components or temporally alternating environments (Models 2a and 2b). First, the evolutionary response to selection differs between the scenarios. In Models 1a and 1b, each generation sees half of the population experiencing selection in each of the two contexts, and the net fitness effect of a mutation is its average between contexts ($s = \frac{1}{2}(s_1 + s_2)$). In contrast, for Models 2a and 2b, the entire population experiences both selection contexts, and net selection across the pair of contexts is approximately the sum of the selection coefficients in each ($s = s_1 + s_2 + s_1 s_2 \approx s_1 + s_2$, when selection coefficients are small). Second, balancing selection can arise in Models 1a and 1b but not 2a and 2b. This distinction is only pertinent to the haploid models we

consider, as balancing selection arises more readily in diploid versions of Fisher's geometric model (see Sellis et al. 2011; Manna et al. 2011; Connallon and Clark 2014b; McDonough et al. 2024).

Because of the different definitions of net selection in Models 1a,b vs. Models 2a,b, the distribution of net fitness effects for new (and established) beneficial mutations is broader for Models 2a,b than Models 1a,b, resulting in a correspondingly higher mean selection coefficient for Models 2a,b (Fig. 5A; see Supplementary Material Appendix 2). However, the probability of exhibiting a trade-off, conditioned on the net-beneficial fitness effect of the mutation, declines more rapidly with s in Models 1a,b than Models 2a,b (Fig. 5A). The differences between models in the distribution of s and the conditional probabilities of trade-offs offset one another, so that the total probability of a trade-off is roughly the same between the models (Fig. 5B).

{Figure 5}

Discussion

Population genetic models of adaptation have played important roles in framing the questions we ask about the genetic basis of evolutionary change, and (in some cases) resolving debates about the types of genetic variants that are likely to be important in evolution (*e.g.*, Kimura 1983; Orr and Coyne 1992; Rockman 2012; Matuszewski et al. 2014, 2015; Bomblies and Peichel 2022; Hayward and Sella 2022). How do trade-offs fit into genetic theories of adaptation? Studies based on Fisher's geometric model have been particularly influential in this regard (Orr 2005a, 2005b; Tenaillon 2014; Connallon and Hodgins 2021). Recent applications of Fisher's geometric model to environments that vary across time, space, life-history stage, or sex, suggest that trade-offs are all but guaranteed to arise under even modest differences in the direction of selection across environments (Moorad and Promislow 2008; Moorad and Hall 2009; Martin

and Lenormand 2015; Connallon and Clark 2014a, 2014b, 2015). However, while previous models have considered the consequences of trade-offs between environments for the rate of adaptation (Martin and Lenormand 2015; Marshall and Connallon 2023) or the probability of evolutionary rescue (Mohammadi and Campos 2025), none have asked the next obvious question: to what extent do mutations exhibiting trade-offs contribute to adaptation?

We have shown that beneficial mutations exhibiting trade-offs tend to have small net effects on fitness, which makes them particularly prone to loss due to genetic drift. Consequently, mutations contributing to adaptation are substantially less likely to exhibit trade-offs than the overall pool of mutations with net-beneficial fitness effects. We have further demonstrated that changes in population size alter the proportion of adaptive substitutions that exhibit trade-offs. Specifically, population size expansions increase, whereas population declines decrease, the contribution of trade-off alleles to adaptation. These effects arise because population size change can both diminish (in expanding populations) or amplify (in declining ones) genetic drift-induced losses of rare adaptive variants (Otto and Whitlock 1997). One implication of these results is that populations experiencing declines, due to habitat degradation or other sources of environmental stress, should largely adapt by fixing alleles that are unconditionally beneficial. In contrast, expanding populations—such as those moving into new ranges—will accumulate alleles that are conditionally beneficial and likely to carry costs in some environments or fitness components. Adaptation is, of course, constrained in declining populations, not only because of the escalation of drift, but also because of the decreasing pool of adaptive alleles that remain segregating, and the diminishing rate of input of novel mutations. Populations able to surpass these challenges (*e.g.*, through 'evolutionary rescue'; Orr and Unckless 2014; Bell 2017; Draghi et al. 2024) are therefore expected to carry alleles that are universally rather than conditionally favourable.

Empirically dissecting the genetic basis of adaptation may be more tractable in populations adapting during periods of decline, as variants contributing to adaptation are expected to have relatively large phenotypic effects (Osmond et al. 2020; McDonough et al. 2023), generate stronger population

genomic signals (Osmond and Coop 2000), and their effects should be unconditionally beneficial (as shown here). At least some of these attributes notably apply to the intriguing example of evolutionary rescue in Hawaiian cricket populations exposed to invasive parasitic flies that are attracted to the songs of male crickets (Zuk et al. 2006). Here, rescue has occurred by the spread of a major quantitative trait locus that eliminates song (Pascoal et al. 2020), which has opened the door for new types of courtship adaptations to evolve (Gallagher et al. 2024). Genomic studies that contrast native versus invasive populations of a species provide further opportunities of testing how population size changes affect the genetics of adaptation. The combination of population genomic scans for selection and association tests for the phenotypes of candidate loci (see Battlay et al. 2023) can be used to test whether systematically different types of variants contribute to the adaptation of native populations relative to invasive populations that have a recent history of population growth.

A corollary to our results applies to structured populations that are subject to gene flow and selection for local adaptation. Gene flow causes the evolutionary dynamics of locally beneficial alleles to at least partially depend on their fitness effects in other regions of the species' range (see Yeaman and Otto 2011). Under high gene flow, the mutations able to establish should tend to be strongly beneficial in regions where they are favoured and carry weak or negligible costs in regions where they are not. In other words, migration places a filter on the types of mutations that contribute to local adaptation. Our results for Model 1b provide predictions for cases where migration is high enough to prevent stable genetic differentiation between populations (*i.e.*, our results represent a high-migration limit). In this limit, evolutionarily successful alleles tend to be beneficial in multiple locations across the range or, at minimum, closer to the ideal of conditional neutrality (*i.e.*, alleles that pose no harm; Martin and Lenormand 2015; Mee and Yeaman 2019) in locations where they are disfavoured. In contrast, populations with high genetic isolation from others (*i.e.*, where migration among populations is low) can adapt using the full spectrum of genetic variants that are locally adaptive, regardless of their potential costs when expressed in other environments (for analyses of Fisher's geometric model with low or no gene flow between habitats, see Thompson et al

2019; Mohammadi and Campos 2025). Consequently, the mutations contributing to local adaptation in structured populations with low gene flow should more often show trade-offs between habitats relative to what we see in our analysis. Despite much evidence for trade-offs in empirical studies of local adaptation (Hereford 2009), this specific hypothesis remains untested at broad taxonomic scale.

Our analysis also clarifies how population dynamics and the geometry of selection between environments influence the likelihood of trade-offs among individual steps of an adaptive walk towards the population's long-term evolutionary equilibrium (in our models, the long-term equilibrium is the phenotype exactly midway between the two optima; $\mathbf{O}_{eq.} = (\mathbf{O_1} + \mathbf{O_2})/2$)). Previous models of adaptive walks with multiple optima predict that the distance to each optimum will shrink over time (both z_1 and z_2 decline), while the angle between selection orientations will increase (*i.e.*, $\cos(\theta_{sel})$ decreases; see Connallon and Clark 2014a; Martin and Lenormand 2015; Marshall and Connallon 2023). Thus, the prevalence of trade-offs should increase among both new *and* established mutations during the time-course of an adaptive walk, though trade-offs should always remain more common among new relative to established adaptive variants at any time point during the walk. If adaptation also leads to population growth and stability—as it would in cases involving evolutionary rescue—this will further increase the prevalence of trade-offs contributing to the later relative to the earlier phases of the adaptive walk, owing to the higher establishment probabilities of trade-off mutations in stable or growing populations relative to declining ones.

Our study leaves open the important question of how common trade-offs might be in cases where adaptation relies on standing genetic variation rather than new mutations, which is an area for future work. Although a full theoretical analysis of this question is beyond the scope of the current paper, there is at least one good reason to expect trade-offs to become more prevalent in cases where adaptation uses standing genetic variation. Previous theory clearly shows that mutations with small phenotypic effects experience relatively weaker selection than those with moderate-to-large effects. Small-effect mutations should, therefore, be enriched in the standing genetic variation that potentially contributes to adaptation in new environments (de Vladar and Barton 2016; Hayward and Sella 2022), enhancing their prospects for

contributing to adaptation in altered environments. And indeed, the effect sizes of genetic variants that contribute to adaptation are predicted to be smaller when adaptation uses standing variation relative to when it uses new mutations (see Matuszewski et al. 2015). We have shown that mutations with small net effects on fitness are the most likely variants to exhibit trade-offs (note that this prediction applies whether the net fitness effect of the mutation is positive or negative; see Supplementary Material Appendix 3). Thus, any enrichment of small-effect alleles in the pool of standing genetic variation would presumably cause enrichment of trade-offs in the alleles that contribute to adaptation from standing genetic variation, following a change in environment.

Our focus on haploid populations applies to microbial, animal and plant species where selection occurs in haploid stages of the life cycle (see Joseph and Kirkpatrick 2004; Immler 2019). What our models overlook is the far greater potential for mutations to experience balancing selection (selection that maintains genetic polymorphism) in predominantly diploid populations. In haploids, conditions leading to balancing selection are restrictive, and variants contributing to adaptation are therefore expected to sweep to fixation (exceptions have been noted for Models 1a and 1b). In contrast, conditions for balancing selection can be permissive in diploid versions of Fisher's geometric model, leading to short-lived episodes of balancing selection that transiently inflate genetic variation within the population (see Sellis et al. 2011; Manna et al. 2011; Connallon and Clark 2014b). To the extent that balancing selection does occur in diploids, adaptive genetic variants may exhibit partial selective sweeps, and balancing polymorphisms may contribute to rapid adaptation under new environmental conditions (Sellis et al. 2011), as implied by recent field data from *Drosophila* and other species (reviewed in Johnson et al. 2023). A detailed characterization of the prevalence of trade-offs in these more complicated scenarios of adaptation is an important task for future research.

Data availability

Simulation code is available at: https://doi.org/10.5281/zenodo.15036232.

Author contributions

Project conceptualization: all authors. Development and analysis of the mathematical model: TC, PC, CO. Computer simulations: LD, DG, HK, ANB, SN, FR, EIS, MKZ. Wrote the manuscript: TC. Edited the manuscript: all authors.

Funding: Support for this research came from the European Society of Evolutionary Biology (ESEB) through a 'Special Topics Network' grant. Further financial support came from the European Research Council (ERC-2023-STG916 #101117517, to CO), the Swedish Research Council (#2022-03603, to CO; #2020- 03123, to EIS), the Research Council of Norway (Norges forskningsråd #302619, to DG), the Alexander von Humboldt Foundation and the GenEvo graduate school (to HK), the Foundation for Zoological Research and the Birgitta Sintring Foundation (#S2024-0007, to MKZ), a postdoctoral fellowship from the Consejo Nacional de Humanidades, Ciencias y Tecnología (to ANB), and a H2020 Marie Skłodowska-Curie COFUND Action fellowship (#101034413, to FR).

Conflict of interest: TC and CO are members of the editorial board for *Evolution*; the editorial process of the manuscript was done independently of TC and CO. PC, DG, HK, ANB, SN, EIS, MKZ, LD, and FR declare no conflict of interest.

Acknowledgements: We wish to express our deepest gratitude to Lotte de Vries for extensive discussion of the project from its conception, rederiving some of our results, and providing comments on an earlier version of the manuscript, and to the European Society of Evolutionary Biology (ESEB) for a 'Special Topics Network' grant that supported workshops that initiated this collaboration and facilitated many new ideas and friendships. We also thank two anonymous reviewers for their thoughtful comments and suggestions that helped us to substantially improve upon the original version of the paper.

References

Aguirre JD, Blows MW, Marshall DJ. 2014. The genetic covariance between life cycle stages separated by metamorphosis. *Proc Roy Soc B* 281:20141091.

Aidoo M, et al. 2002. Protective effects of the sickle cell gene against malaria morbidity and mortality. *The Lancet* 359:1311-1312.

Anciaux Y, Chevin LM, Ronce O, Martin G. Evolutionary rescue over a fitness landscape. *Genetics* 209:265-279.

Anderson JT, Lee CR, Rushworth CA, Colautti RI, Mitchell-Olds T. 2013. Genetic trade- offs and conditional neutrality contribute to local adaptation. *Molecular Ecology* 22:699-708.

Arnold SJ, Wade MJ. 1984. On the measurement of natural and sexual selection: Theory. *Evolution* 38:709-719.

Barson NJ, Aykanat T, Hindar K, Baranski M, Bolstad GH, Fiske P, Jacq C, Jensen AJ, Johnston SE, Karlsson S, Kent M, Moen T, Niemelä E, Nome T, Naesje TF, Orell P, Romakkaniemi A, Saegrov H, Urdal K, Erkinaro J, Lien S, Primmer CR. 2015. Sex-dependent dominance at a single locus maintains variation in age at maturity in salmon. *Nature* 528:405-408.

Battlay P, et al. 2023. Large haploblocks underlie rapid adaptation in the invasive weed *Ambrosia artemisiifolia*. *Nature Communications* 14:1717.

Bell G. 2017. Evolutionary rescue. *Ann Rev Ecol Evol Syst*. 48:605-627.

Bergland AO, Behrman EL, O'Brien KR, Schmidt PS, Petrov DA. 2014. Genomic evidence of rapid and stable adaptive oscillations over seasonal time scales in Drosophila. *PLoS Genet*. 10:e1004775.

Bitter MC, Berardi S, Oken H, Huynh A, Lappo E, Schmidt P, Petrov DA. 2024. Continuously fluctuating selection reveals fine granularity of adaptation. *Nature* in press.

Bomblies K, Peichel CL. 2022. Genetics of adaptation. *Proc Natl Acad Sci USA* 119:e2122152119.

Charlesworth B. 2015. The causes of natural variation in fitness: Evidence from studies of *Drosophila*. *Proc Natl Acad Sci USA* 112:1662-1669.

Charlesworth B, Charlesworth D. 1978. A model for the evolution of dioecy and gynodioecy. *Am Nat.* 112:975-997.

Charlesworth B, Hughes KA. 2000. The maintenance of genetic variation in life history traits. In Singh RS, Krimbas CB (eds.) *Evolutionary Genetics: from Molecules to Morphology*, pp. 369-391. Cambridge University Press: Cambridge, UK.

Christiansen FB. 1975. Hard and soft selection in a subdivided population. *Am Nat*. 109:11-16.

Connallon T, Clark AG. 2014a. Evolutionary inevitability of sexual antagonism. *Proc Roy Soc B* 281:20132123.

Connallon T, Clark AG. 2014b. Balancing selection in species with separate sexes: insights from Fisher's geometric model. *Genetics* 197:991-1006.

Connallon T, Hall MD. 2018. Genetic constraints on adaptation: a theoretical primer for the genomics era. *Annals NY Acad Sciences* 1422:65-87.

Connallon T, Hodgins KA. 2021. Allen Orr and the genetics of adaptation. *Evolution* 75:2624-2640.

Connallon T, Sharma S, Olito C. 2019. Evolutionary consequences of sex-specific selection in variable environments: four simple models reveal diverse evolutionary outcomes. *Am Nat.* 193:93-105.

Cook LM. 2003. The rise and fall of the Carbonaria form of the peppered moth. *The Quarterly Review of Biology* 78:399-417/

Crow JF, Kimura M. 1970. *An introduction to population genetics theory*. Harper and Row, New York.

Curtsinger JW, Service PM, Prout T. 1994. Antagonistic pleiotropy, reversal of dominance, and genetic polymorphism. *Am Nat*. 144:210–228.

de Vladar HP, Barton N. 2016. Stability and response of polygenic traits to stabilizing selection and mutation. *Genetics* 197:749-767.

Dempster E. 1955. Maintenance of genetic heterogeneity. *Cold Spring Harbor Symposia on Quantitative Biology* 20:25-32.

Draghi JA, McGlothlin JW, Kindsvater HK. 2024. Demographic feedbacks during evolutionary rescue can slow or speed adaptive evolution. *Proc Roy Soc B* 291:20231553.

Felsenstein J. 1976. The theoretical population genetics of variable selection and migration. *Annu Rev Genet.* 10:253-280.

Fisher RA. 1930 *The Genetical Theory of Natural Selection*. Oxford University Press: Oxford.

Flatt T. 2020. Life-History evolution and the genetics of fitness components in *Drosophila melanogaster*. *Genetics* 214:3-48.

Fry JD. 1996. The evolution of host specialization: are trade-offs overrated? *Am Nat.* 148:S84-S107.

Futuyma DJ, Moreno G. 1988. The evolution of ecological specialization. *Annu Rev Ecol Syst*. 19:207-233

Gallagher JH, Broder ED, Wikle AW, O'Toole H, Durso C, Tinghitella RM. 2024. Surviving the serenade: how conflicting selection pressures shape the early stages of sexual signal diversification. *Evolution* 78:835-848.

Gardner A. 2024. A geometric approach to the evolution of altruism. *J Theor Biol*. 576:111653.

Gillespie JH. 1984. Molecular evolution over the mutational landscape. *Evolution* 38:1116-1129.

Glaser- Schmitt A, Ramnarine TJS, Parsch J. 2024. Rapid evolutionary change, constraints and the maintenance of polymorphism in natural populations of *Drosophila melanogaster*. *Molecular Ecology* 33:e17024.

Gliddon C, Strobeck C. 1975. Necessary and sufficient conditions for multiple-niche polymorphism in haploids. *Am Nat.* 109:233-235.

Goedert D, Calsbeek R. 2019. Experimental evidence that metamorphosis alleviates genomic conflict. Am Nat. 194:356-366.

Gregorius HR. 1982. Selection in diplo-haplonts. *Theor Pop Biol*. 21:289-300.

Haldane JBS. 1927. A mathematical theory of natural and artificial selection, part V: selection and mutation. *Proc Camb Philos Soc*. 28:838–844.

Haldane JBS. 1937. The effect of variation on fitness. *Am Nat.* 71:337-349.

Hayward LK, Sella G. 2022. Polygenic adaptation after a sudden change in environment. *Elife* 11:e66697

Hereford J. 2009. A quantitative survey of local adaptation and fitness trade-offs. *Am Nat*. 173:579-588.

Hermisson J, Redner O, Wagner H, Baake E. 2002. Mutation–selection balance: ancestry, load, and maximum principle. *Theor Pop Biol*. 62:9-46.

Immler S. 2019. Haploid selection in "diploid" organisms. *Annu Rev Ecol Evol Syst*. 50:219-236.

Johnson OL, Tobler R, Schmidt JM, Huber CD. 2023. Fluctuating selection and the determinants of genetic variation. *Trends in Genetics* 39:491–504.

Johnston SE, Gratten J, Berenos C, Pilkington JG, Clutton-Brock TH, Pemberton JM, Slate J. 2013. Life history trade-offs at a single locus maintain sexually selected genetic variation. *Nature* 502:93-95.

Joseph SB, Kirkpatrick M. Haploid selection in animals. *Trends Ecol Evol*. 19:592-597.

Kawecki TJ, Ebert D. 2004. Conceptual issues in local adaptation. *Ecology Letters* 7:1225-1241

Kidwell JF, Clegg MT, Stewart FM, Prout T. 1977. Regions of Stable equilibria for models of differential selection in the two sexes under random mating. *Genetics* 85:171–183.

Kimura M. 1962. On the probability of fixation of mutant genes in a population. *Genetics* 47:713–719.

Kimura M. 1983. *The Neutral Theory of Molecular Evolution*. Cambridge University Press: Cambridge.

Kopp M, Hermisson J. 2009. The genetic basis of phenotypic adaptation II: the distribution of adaptive substitutions in the moving optimum model. *Genetics* 183:1453-1476.

Kreider JJ, Pen I, Kramer BH. 2021. Antagonistic pleiotropy and the evolution of extraordinary lifespans in eusocial organisms, *Evol Letters* 5:178-186

Lande R. 1980. Sexual dimorphism, sexual selection, and adaptation in polygenic characters. *Evolution* 34:292-305.

Lehtonen J. 2020. Longevity and the drift barrier: Bridging the gap between Medawar and Hamilton. *Evol Letters* 4:382-393.

Lemaître JF, Moorad JA, Gaillard J-M, Maklakov AA, Nussey DH. 2024. A unified framework for evolutionary genetic and physiological theories of aging, *PLoS Biology* 22:e3002513.

Lenormand T, Harmand N, Gallet R. 2018. Cost of resistance: an unreasonably expensive concept. *Rethinking Ecology* 3:51-70.

Levene H. 1953. Genetic equilibrium when more than one ecological niche is available. *Am Nat*. 87:331-333.

Mangan R, Bussière LF, Polanczyk RA, Tinsley MC. 2023. Increasing ecological heterogeneity can constrain biopesticide resistance evolution. *Trends Ecol Evol*. 38:605-614.

Manna F, Martin G, Lenormand T. 2011. Fitness landscapes: an alternative theory for the dominance of mutation. *Genetics* 189:923-937.

Marshall DJ, Connallon T. 2023. Carry- over effects and fitness trade- offs in marine life histories: The costs of complexity for adaptation. *Evol Applications* 16:474-485.

Martin G, Lenormand T. 2006a. A general multivariate extension of Fisher's geometrical model and the distribution of mutation fitness effects across species. *Evolution* 60:893-907.

Martin G, Lenormand T. 2006b. The fitness effect of mutations across environments: a survey in light of fitness landscape models. *Evolution* 60:2413-2427.

Martin G, Lenormand T. 2008. The distribution of beneficial and fixed mutation fitness effects close to an optimum. *Genetics* 179:907-916.

Martin G, Lenormand T. 2015. The fitness effect of mutations across environments: Fisher's geometrical model with multiple optima. *Evolution* 69:1433-1447.

Matuszewski S, Hermisson J, Kopp M. 2014. Fisher's geometric model with a moving optimum. *Evolution* 68:2571-2588.

Matuszewski S, Hermisson J, Kopp M. 2015. Catch me if you can: adaptation from standing genetic variation to a moving phenotypic optimum. *Genetics* 200:1255-1274

Maynard Smith J. 1970. Natural selection and the concept of a protein space. *Nature* 225:563-564.

McCandlish DM, Stoltzfus A. 2014. Modeling evolution using the probability of fixation: history and implications. *Quarterly Review of Biology* 89:225-252.

McDonough Y, Connallon T. 2023. Effects of population size change on the genetics of adaptation following an abrupt change in environment. *Evolution* 77:1852-1863.

McDonough Y, Ruzicka F, Connallon T. 2024. Reconciling theories of dominance with the relative rates of adaptive substitution on sex chromosomes and autosomes. *Proc Natl Acad Sci USA* 121:e2406335121.

Medawar PB. 1952. *An Unsolved Problem of Biology*. H. K. Lewis and Company: London.

Mee JA, Yeaman S. 2019. Unpacking Conditional neutrality: Genomic signatures of selection on conditionally beneficial and conditionally deleterious mutations. *Am Nat*. 194:529-540.

Mohammadi A, Campos PRA. 2025. Geometric insights into evolutionary rescue dynamics in a two-deme model. *Evolution*, in press.

Moorad JA, Hall DW. 2009. Age-dependent mutational effects curtail the evolution of senescence by antagonistic pleiotropy. *J Evol Biol*. 22:2409-2419.

Moorad JA, Promislow DEL. 2008. A theory of age-dependent mutation and senescence. *Genetics* 179:2061-2073.

Moutinho AF, Eyre-Walker A, Dutheil JY. 2022. Strong evidence for the adaptive walk model of gene evolution in Drosophila and Arabidopsis. *PLoS Biol*. 20:e3001775.

Moran NA. 1994. Adaptation and constraint in the complex life cycles of animals. *Annu Rev Ecol Syst*. 25:573-600.

Orr HA. 1998. The population genetics of adaptation: The distribution of factors fixed during adaptive evolution. *Evolution* 52:935–949.

Orr HA. 2000. Adaptation and the cost of complexity. *Evolution* 54:13-20.

Orr HA. 2005a. The genetic theory of adaptation: A brief history. *Nat Rev Genet*. 6:119–127.

Orr HA. 2005b. Theories of adaptation: what they do and don't say. *Genetica* 123:3–13.

Orr HA, Coyne JA. 1992. The genetics of adaptation: A reassessment. *Am Nat*. 140:725–742.

Orr HA, Unckless RL. 2014. The population genetics of evolutionary rescue. *PLoS Genetics* 10:e1004551.

Osmond MM, Coop G. 2020. Genetic signatures of evolutionary rescue by a selective sweep. *Genetics* 215:813-829.

Osmond MM, Otto SP, Martin G. 2000. Genetic paths to evolutionary rescue and the distribution of fitness effects along them. *Genetics* 214:493-510.

Otto SP, Whitlock MC. 1997. The probability of fixation in populations of changing size. *Genetics* 146:723-733.

Pascoal S, Risse JE, Zhang X, Blaxter M, Cezard T, Challis RJ, Gharbi K, Hunt J, Kumar S, Langan E, Liu X, Rayner JG, Ritchie MG, Snoek BL, Trivedi U, Bailey NW. 2020. Field cricket genome reveals the footprint of recent, abrupt adaptation in the wild. *Evolution* Letters 4:19-33.

Pennell, TM, Mank JE, Alonzo SH, Hosken DJ. 2024. On the resolution of sexual conflict over shared traits. *Proc Roy Soc B* 291:20240438.

Prout T. 2000. How well does opposing selection maintain variation? In Singh RS, Krimbas CB (eds.) *Evolutionary Genetics: From Molecules to Morphology*, pp. 157–181. Cambridge University Press: Cambridge, UK.

R Core Team. (2021). *R: A language and environment for statistical computing*. R Foundation for Statistical Computing.

Rockman MV. 2012. The QTN program and the alleles that matter for evolution: all that's gold does not glitter. *Evolution* 66:1-17.

Rousselle M, Simion P, Tilak MK, Figuet E, Nabholz B, Galtier N. 2020. Is adaptation limited by mutation? A timescale-dependent effect of genetic diversity on the adaptive substitution rate in animals. *PLoS Genet.* 16:e1008668.

Rusuwa BB, Chung H, Allen SL, Frentiu FD, Chenoweth SF. 2022. Natural variation at a single gene generates sexual antagonism across fitness components in Drosophila. *Current Biology* 32:3161-3169.

Ruzicka F, Hill MS, Bennell TM, Flis I, Ingleby FC, Mott R, Fowler K, Morrow EH, Reuter M.2019. Genome-wide sexually antagonistic variants reveal long-standing constraints on sexual dimorphism in fruit flies. *PLoS Biol*. 17:e3000244.

Ruzicka F, Holman L, Connallon T. 2022. Polygenic signals of sex differences in selection in humans from the UK Biobank. *PLoS Biol*. 20:e3001768.

Schneemann H, De Sanctis B, Welch JJ. 2024. Fisher's geometric model as a tool to study speciation. *Cold Spring Harb Perspect Biol*. 16:a041442.

Scott TJ, Queller DC. 2019. Long- term evolutionary conflict, Sisyphean arms races, and power in Fisher's geometric model. *Ecology and Evolution* 9:11243-11253.

Sellis D, Callahan BJ, Petrov DA, Messer PW. 2011. Heterozygote advantage as a natural consequence of adaptation in diploids. *Proc Natl Acad Sci USA* 108:20666-20671.

Tenaillon O. 2014. The utility of Fisher's geometric model in evolutionary genetics. *Annu Rev Ecol Evol Syst*. 45:179-201.

Thompson KA, Osmond MM, Schluter D. 2019. Parallel genetic evolution and speciation from standing variation. *Evolution Letters* 3:129-141.

Williams GC. 1957. Pleiotropy, natural selection, and the evolution of senescence. *Evolution* 11:398–411.

Wittmann MJ, Mousset S, Hermisson J. 2023. Modeling the genetic footprint of fluctuating balancing selection: from the local to the genomic scale. *Mol Biol Evol*. 223:iyad022.

Yamaguchi R, Wiley B, Otto SP. 2022. The phoenix hypothesis of speciation. *Proc Roy Soc B*. 289:20221186.

Yeaman S, Otto SP. 2011. Establishment and maintenance of adaptive genetic divergence under migration, selection, and drift. *Evolution* 65:2123-9.

Wang Z, Liao BY, Zhang J. 2010. Genomic patterns of pleiotropy and the evolution of complexity. *Proc Natl Acad Sci USA* 107:18034-18039.

Zuk M, Rotenberry JT, Tinghitella RM. 2006. Silent night: adaptive disappearance of a sexual signal in a parasitized population of field crickets. *Biology Letters* 2:521–524.

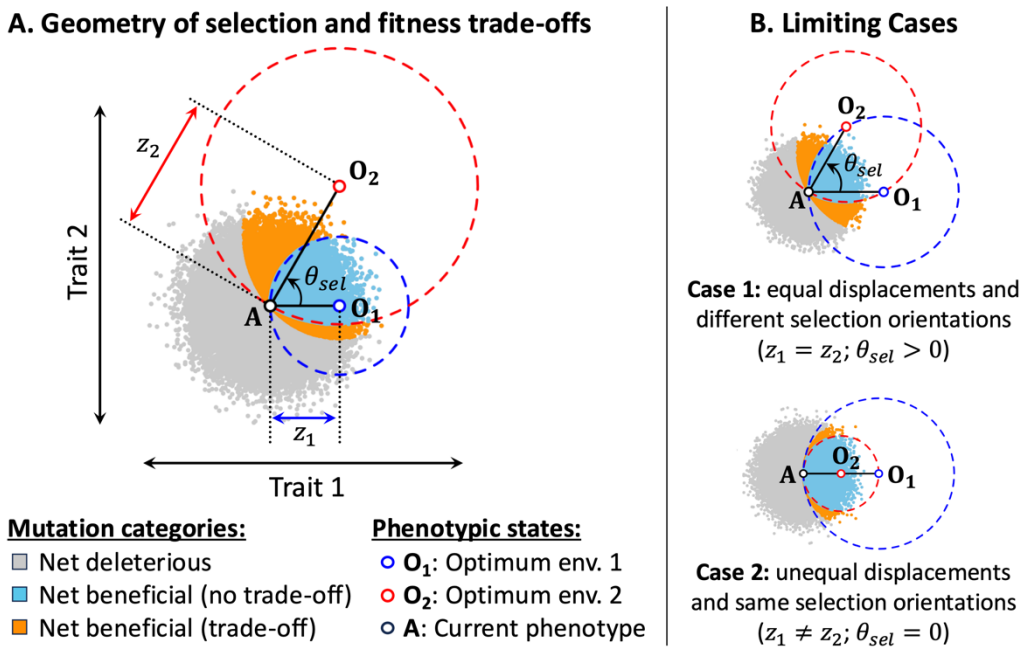

Figure 1. An overview of Fisher's geometric model with two trait dimensions and two environments of selection. **A**, $\mathbf{O_1}$ and $\mathbf{O_2}$ are vectors that represent trait values for the resident genotype (**A**), and optimal phenotypes for environments 1 and 2 ($\mathbf{O_1}$ and $\mathbf{O_2}$); z_1 and z_2 are the distances between resident genotype **A** and optima $\mathbf{O_1}$ and $\mathbf{O_2}$, respectively, and θ_{sel} quantifies misalignment in the direction of displacement from each optimum. **Panel A** illustrates how changes in environment can affect both the distance and the orientation of a population away from its optimum, leading to fitness trade-offs between the environments. The phenotypes of 10^5 random mutations are colour-coded to denote their net fitness effects, with net deleterious mutations in grey, net beneficial mutations in orange (those exhibiting trade-offs) and blue (those that do not). **Panel B** shows two limiting cases of the general model that each predict trade-offs.

ALT TEXT. An illustration of selection and genetic trade-offs between a pair of environments in the Fisher's geometric model framework.

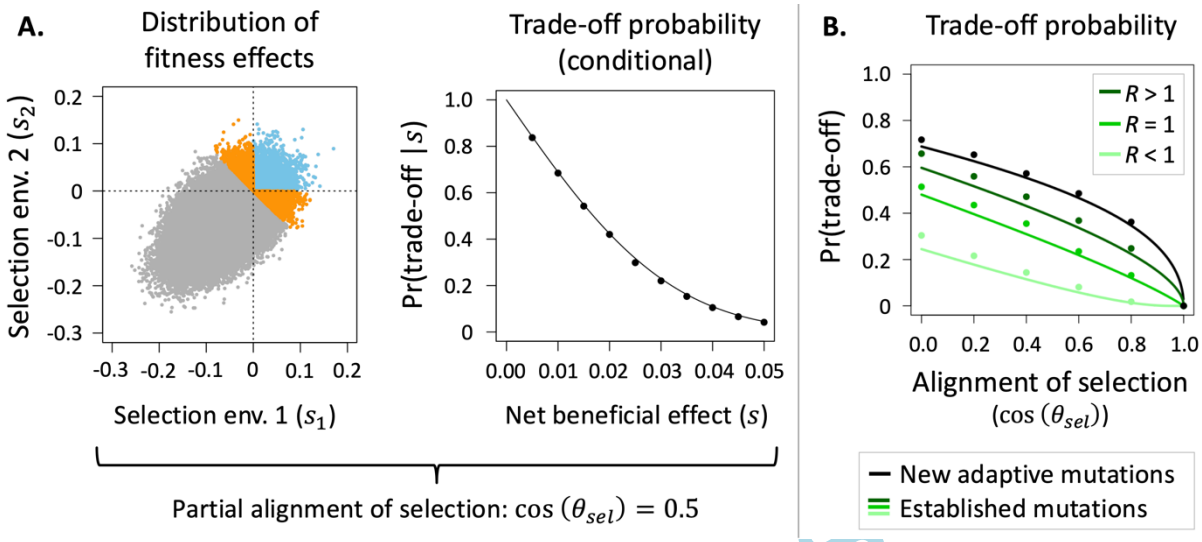

Figure 2. Genetic trade-offs between environments with different orientations of selection ($\cos(\theta_{sel}) < 1$) and equal magnitudes of displacement from the optima ($z_1 = z_2$). Selection differs between a pair of habitats or sexes (selection environments 1 and 2), with $s = (s_1 + s_2)/2$ representing the net fitness effect of a mutation (net-beneficial mutations have $s > 0$). **Part A** shows an example where selection is partially aligned between environments ($\cos(\theta_{sel}) = 0.5$). Dots in the left-hand panel show 10^5 simulated mutations, with net deleterious mutations in grey and net beneficial mutations in orange (which trade-off between environments) and blue (which do not). The right-hand panel shows the relation between the fitness effect of a net-beneficial mutation and its probability of exhibiting a trade-off (the curve is based on eq. (4) and circles are each based on 10^5 simulated mutations). **Part B** shows the proportions of new (black) and established mutations (green shades) that exhibit trade-offs. Curves are based on eqs. (5-6), with $\cos(\theta_{sel})$ spanning the range from orthogonal to completely aligned directions of selection between environments (*i.e.*, $\cos(\theta_{sel}) \in [0, 1]$). Simulation results were calculated from the first 1000 established mutations, with establishments occurring in populations of constant ($R = 1$), increasing ($R = 1.02$), or decreasing ($R = 0.98$) size. Additional parameters are $z = 1$, $m = 0.05$, and $n = 50$. For further results (with different values of n and z) see Fig. S4 of the Supplementary Material. Fig. S6 illustrates how $\cos(\theta_{sel})$ affects the geometry of selection.

ALT TEXT. The predicted proportion of adaptive substitutions exhibiting trade-offs between environments. In this version of the model, the population has an equal displacement from the optimum in each environment, whereas the direction of selection differs between environments.

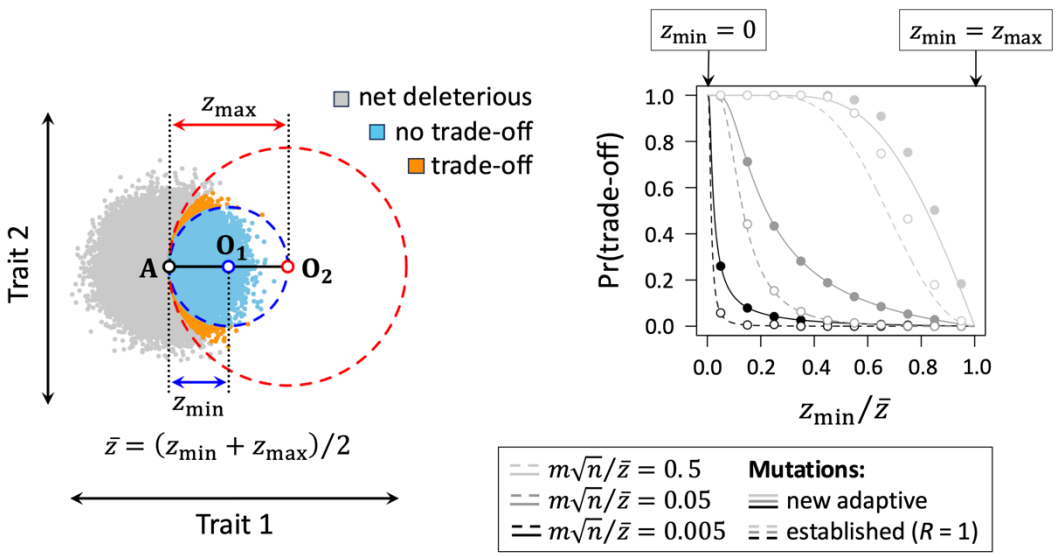

Figure 3. Genetic trade-offs between environments with identical orientations of selection ($\cos(\theta_{sel}) = 1$) and different magnitudes of displacement from the optima ($z_1 \neq z_2$). The left-hand panel shows an example where the population's displacement from the optimum in one environment is half the displacement in the other ($z_{\min} = z_{\max}/2$, where in this case $z_1 = z_{\min}$ and $z_2 = z_{\max}$). Dots denote mutations with net deleterious (grey) and net beneficial effects (orange and blue). The right-hand panel shows the proportion of trade-offs among net beneficial mutations (solid curves and filled circles) and established mutations (broken curves and open circles), with curves based on eqs. (7-8) and each circle based 10^6 simulated mutations. Additional parameters include $\bar{z} = (z_{\min} + z_{\max})/2 = 1$ and n = 50, and establishments occur in populations of constant size (R = 1).

ALT TEXT. The predicted proportion of adaptive substitutions exhibiting trade-offs between environments. In this version of the model, the population has an unequal displacement from the optimum in each environment, whereas the direction of selection is the same between environments.

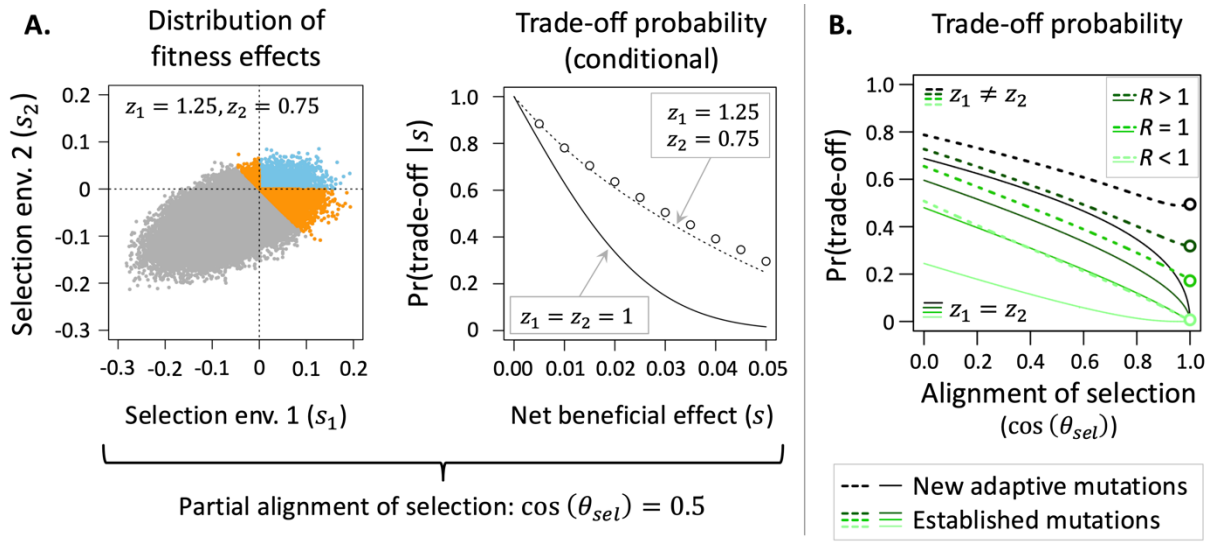

Figure 4. Genetic trade-offs between environments with different orientations of selection ($\cos(\theta_{sel}) < 1$) and asymmetric displacements from the optima ($z_1 \neq z_2$). An example with mildy asymmetric displacements ($z_1 = 1.25$ and $z_2 = 0.75$) is compared with a case involving symmetrical displacements with the same average displacement ($z_1 = z_2 = 1$; note that $\bar{z} = (z_1 + z_2)/2 = 1$ in each case). Curves for the symmetric cases are based on eqs. (5-6), and those for the asymmetric cases are based on eqs. (S11-S12) in the Supplementary material. Circles in panel B show the analytical approximations for the special case where directional selection is perfectly aligned between environments (*i.e.*, $\cos(\theta_{sel}) = 1$, from eqs. (7-8) in the main text and eqs. (S17-S18) in the Supplementary Material). All other details match those of Fig. 2. Fig. S6 illustrates how $\cos(\theta_{sel})$ affects the geometry of selection.

ALT TEXT. The predicted proportion of adaptive substitutions exhibiting trade-offs between environments. In this version of the model, the population has an unequal displacement from the optimum in each environment, and the direction of selection differs between environments.

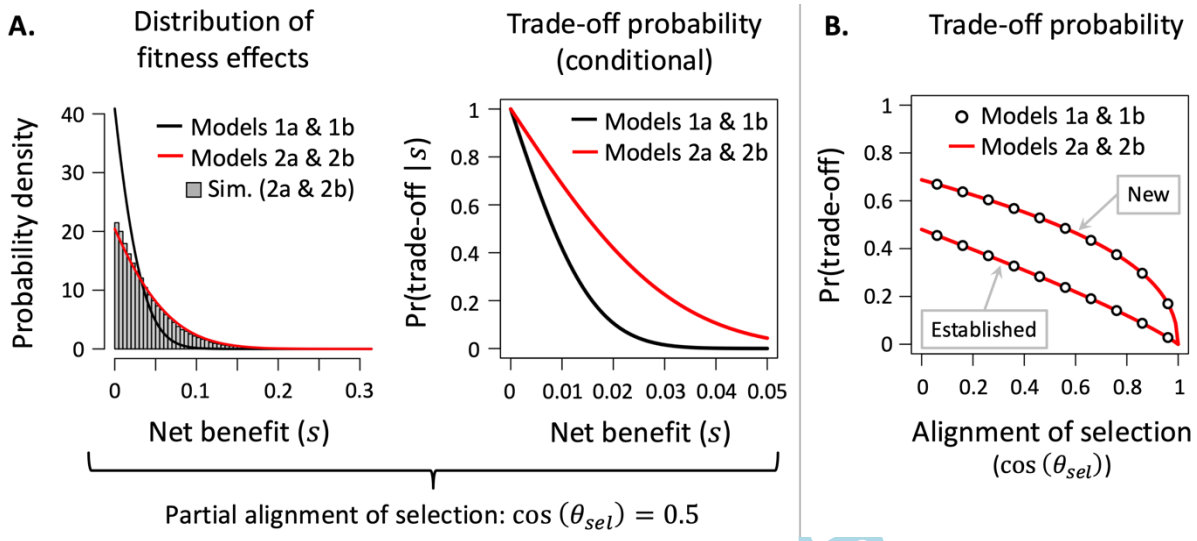

Figure 5. Fitness effects and trade-offs in models of sex- or habitat-specific selection (Models 1a and 1b) and models involving differential selection between fitness components or temporally alternating environments (Models 2a and 2b). Results represent cases where $m = 0.05$, $z_1 = z_2 = 1$, and $n = 50$. **Panel A** shows the distribution of net fitness effects and conditional probabilities of trade-offs when there is intermediate alignment of selection between environments ($\cos(\theta_{sel}) = 0.5$). **Panel B** shows the total probability of trade-offs for new adaptive mutations and for established mutations across a range of orientations of selection between environments ($0 \leq \cos(\theta_{sel}) \leq 1$). The curves are based on equations presented in the Supplementary Material, while histograms are based on simulations of exact fitness effects in Fisher's geometric model. Fig. S6 illustrates how $\cos(\theta_{sel})$ affects the geometry of selection.

ALT TEXT. Comparison of the predictions of different trade-off scenarios.